Forbidden Directions for the Fracture of Thin Anisotropic Sheets: An Analogy with the Wulff Plot

Atsushi Takei, Benoît Roman,* and José Bico
PMMH, UMR 7636 ESPCI/CNRS/UPMC/U.Diderot, 10 rue Vauquelin, 75231 Paris CEDEX 05, France

Eugenio Hamm and Francisco Melo
Departamento de Física, Universidad de Santiago de Chile, Avenida Ecuador 3493, 9170124 Estación Central, Santiago, Chile
(Received 31 January 2013; revised manuscript received 5 March 2013; published 2 April 2013)

It is often postulated that quasistatic cracks propagate along the direction allowing fracture for the lowest load. Nevertheless, this statement is debated, in particular for anisotropic materials. We performed tearing experiments in anisotropic brittle thin sheets that validate this principle in the case of weak anisotropy. We also predict the existence of forbidden directions and facets in strongly anisotropic materials, through an analogy with the description of equilibrium shapes in crystals. However, we observe cracks that do not necessarily follow the easiest direction but can select a harder direction, which is only locally more advantageous than neighboring paths. These results challenge the traditional description of fracture propagation, and we suggest a modified, less restrictive criterion compatible with our experimental observations.

DOI: 10.1103/PhysRevLett.110.144301 PACS numbers: 46.50.+a, 46.70.De, 62.20.mt, 81.70.Bt

Impeding fracture propagation has been the focus of most engineering efforts, with the aim of preventing the ruin of human-built structures. But predicting and controlling the path of a running crack is also important in many applications, from manufacturing of Silicon wafers (obtained by slicing a single crystal) to fracture-induced patterning at nanoscale [1]. The prediction of a crack path along thin sheets is particularly useful in the design of easier-to-open packaging [2–6] or safer oil tanker hulls [7]. Observing a crack path also provides a measurement of the material properties of thin films [2] and even graphene sheets [8]. From a fundamental point of view, the tearing of thin sheets has also received attention because of the remarkable reproducibility of the crack path [2–9] and its intriguing instabilities [3–6]. Previous studies have all assumed an isotropic medium, although most thin materials are anisotropic because of manufacturing process. However, the principles of fracture mechanics do not provide a definite answer to this apparently simple question. Which path will a crack follow through an anisotropic material?

According to Griffith's criterion [10,11], a crack propagates in a direction θ when the energy released per unit of propagation area (the energy release-rate G) balances the surface energy cost of fracturing the material, G_c:

$$G(\theta) = G_c. \tag{1}$$

In the case of an isotropic material, the following two postulates [11] dictate the propagation angle: (i) By symmetry, cracks propagate in the direction where mode II is absent from the stress field near the crack tip (principle of local symmetry (PLS) [12]); (ii) Cracks propagate in the first direction that satisfies Griffith's criterion for an imposed load (maximum energy release rate (MERR) [13]). Both principles are equivalent except at a singular kinking point [14–16]. Consider now an anisotropic material whose fracture energy $G_c(\theta)$ is a function of the direction of propagation. Although PLS is not relevant any more, MERR can be extended naturally [16–19]. Griffith's criterion is first reached in the direction

$$\theta \text{ such that } G(\theta)/G_c(\theta) \text{ is globally maximal.} \tag{2}$$

When the derivatives exist, the combination of (1) and (2) leads to $dG/d\theta = dG_c/d\theta$, which can be interpreted as an Eshelby torque balance [19]. This variational criterion has been formalized recently [16,18] and tested numerically on phase-field models of fracture [18,19]. We propose to experimentally study the tearing of a sheet in a "trouser-test" mode III configuration (Fig. 1). To interpret our results in both weakly and strongly anisotropic sheets, we shall translate this criterion into a simple geometric construction analogous to a Wulff's plot for crystal growth. In particular, we shall give evidence of missing directions along which the material never tears, a feature until now specific to crystals.

Our experiments consist of pulling the tabs of a strip (20-mm wide and 100-mm long) precut along a direction inclined by α with the axis of the sheet (Fig. 1). We use two types of bioriented polypropylene sheets of equal thickness (50 μm) but different degrees of anisotropy. Biaxial stretching during extrusion generally leads to strong anisotropy of the material (case of material B, with Young's modulus varying from 1.9 to 3.4 GPa depending on the direction). But we also used a "balanced" material which exhibits weak anisotropy (material A, Young's modulus with less than 20% variation around 1.8 GPa). In the following, $\theta = 0$ corresponds to propagation perpendicular to extrusion direction. Both materials can be modeled [3,4] as brittle [20]. The tabs are clamped in jaws (see Fig. 1)

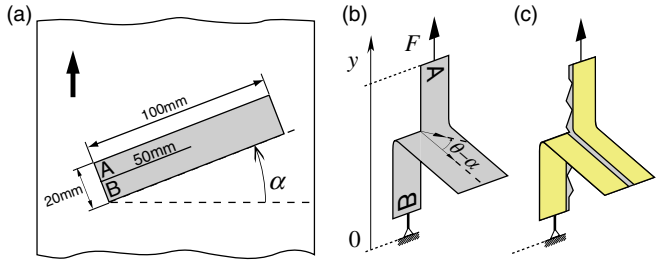

FIG. 1 (color online). Trouser-test experiment. (a) Sample with a starting cut of orientation α. The arrow indicates the sheet axis. (b) The fracture propagates for an applied force F with a deflection angle $\theta - \alpha$. (c) Guided strip experiment (reinforcement in yellow).

displaced with imposed pulling speed 50 mm/min, and the corresponding force is monitored with a load cell with a resolution of 0.6 mN. As the tabs are pulled apart, the crack propagates along a straight path, in direction θ. For an isotropic material [21], the symmetry of the system imposes a propagation in the direction of tearing ($\theta = \alpha$). This symmetry is broken in the case of an anisotropic material. For a material with weak anisotropy (material A), small deviations $\theta - \alpha$ are indeed observed [Fig. 2(a)], while the propagation angle θ still spans all possible directions. In addition, we observe eight specific directions where $\theta = \alpha$. Conversely, in a strongly anisotropic material (material B), four angular sectors are missing [Fig. 2(b)].

To interpret these results, we consider the sheet as inextensible and neglect the bending energy involved in the folds that develop from pulling (see Supplemental Material for justification [22]). The energy release-rate G therefore reduces to the rate of work per unit of surface created, $G(\theta)tds = Fdy$, where t is the thickness of the sheet and F the force applied as the crack advances by ds. Since geometry imposes $dy = 2\cos(\theta - \alpha)ds$, we obtain

$$G(\theta) = 2(F/t)\cos(\theta - \alpha). \tag{3}$$

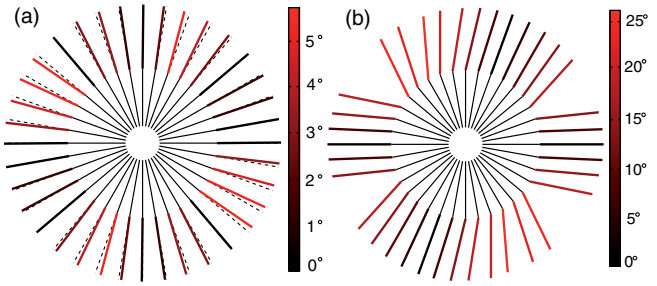

FIG. 2 (color online). Tearing of (a) weakly (material A) and (b) strongly anisotropic sheets (material B), where missing directions are evidenced. The direction of propagation θ (in colored thick lines) when tearing in direction α (thin and dashed lines) is represented in a rosace. Color codes indicate the amplitude of deflection $|\theta - \alpha|$.

Note that $G(\theta)$ is independent of the (possibly anisotropic) elastic properties of the material. Our configuration thus provides a convenient test for bidimensional geometries, where only anisotropy in fracture energy is considered, in contrast with previous studies in anisotropic bulk fracture [23].

We use a simple graphical construction to predict the direction of propagation θ for the tearing orientation α according to Eqs. (1)–(3). We plot in polar coordinates $1/G_c(\theta)$, which we refer to as the G_c^{-1} curve, and $1/G(\theta) = [2(F/t)\cos(\theta - \alpha)]^{-1}$, which corresponds to a straight line oriented along the direction $\alpha + \pi/2$, at a distance $t/2F$ from the origin (see Fig. 3). As F increases, this line comes closer to the origin, keeping its orientation. Griffith's criterion (1) is satisfied at any intersection of the line with the G_c^{-1} curve. According to the maximization criterion (2), propagation occurs at the first intersection (the tangent), defining the tearing force and the direction of propagation.

In the case of an isotropic material, the G_c^{-1} curve is a circle [Fig. 3(a)], and the propagation follows the direction of tearing $\theta = \alpha$. In contrast, when anisotropy is present, the G_c^{-1} curve is noncircular, and the following three different situations may occur: (i) If the curve is locally smooth, the tangential contact point gives, in general, a propagation along a direction $\theta \neq \alpha$. The crack is deflected towards a direction of lower fracture energy. (ii) If the G_c^{-1} curve exhibits a cusp [Fig. 3(c)], the corresponding fracture direction θ_f will be selected for a finite range of loading orientations $\alpha_- < \alpha < \alpha_+$. This situation is reminiscent of cleavage planes in crystals [23–25]. (iii) If the G_c^{-1} curve is locally nonconvex, a finite jump in the direction of propagation $\theta(\alpha)$ is observed as α is varied continuously [Fig. 3(d)]. As a result, the directions $\theta_- < \theta < \theta_+$ cannot be selected through the trouser-test method and will correspond to forbidden angles. The bounding angles θ_- and θ_+ are readily determined with a double-tangent construction, as in classical Maxwell construction.

A similar geometrical construction, referred to as Wulff's plot, is used to predict the equilibrium shape of a crystal with an anisotropic surface tension $\gamma(\theta)$ [26,27] The polar curve $1/\gamma(\theta)$ is denoted as the γ^{-1} curve. In this

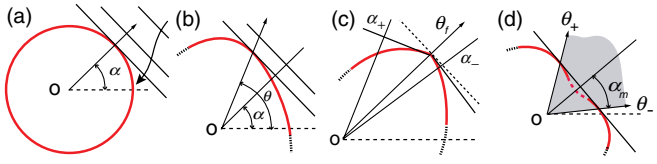

FIG. 3 (color online). Geometrical representation of the global criterion for fracture propagation [Eqs. (1) and (2)]. The crack propagates at the first intersection of the parallel (black) lines (representing G) with the G_c^{-1} curve (in red). (a) Isotropic case, the arrow indicates increasing force; (b) weakly anisotropic case; (c) singular anisotropy leading to facet; (d) anisotropy leading to "forbidden orientations" (grey sector).

context, the point with the polar angle θ on the segment that joins any two points (θ_a, θ_b) of the γ^{-1} curve corresponds to the surface energy of a sawtooth surface constructed with alternating local orientation θ_a and θ_b, averaging to the same global orientation θ. If this point lies inside of the γ^{-1} curve, the flat surface oriented along θ has a lower surface energy than the sawtooth structure and is therefore energetically favorable. All orientations are thus stable if the γ^{-1} curve is convex. Conversely, if the γ^{-1} curve exhibits a nonconvex part, the same convexification construction as in Fig. 3(d) defines a range of unstable (or forbidden) orientations. The expression for the curvature in polar coordinates reads $(\gamma'' + \gamma)/[(\gamma'/\gamma)^2 + 1]^{3/2}$. Nonconvexity therefore occurs when

$$s(\theta) = \gamma''(\theta) + \gamma(\theta) < 0. \quad (4)$$

The quantity $s(\theta)$ is referred to as surface stiffness in crystallography literature [28]. In practice, if a surface is prepared with an orientation in a forbidden direction, the surface reorganizes through spinodal decomposition into alternating orientations θ_-, θ_+ determined by the double-tangent construction [29]. This instability known as faceting generates tunable nanoscaled sawtooth structures on solid crystals [30,31] and was also observed on liquid crystals [32–34]. Note that the forbidden sector $[\theta_-, \theta_+]$ is wider than the region with negative curvature [where $s(\theta) < 0$, see Fig. 3(d)]. Some orientations with $\theta_- < \theta < \theta_+$ but $s(\theta) > 0$ are therefore expected to be metastable, just like supercooled gas or superheated liquid near the first-order liquid-gas transition. We can translate classical results from the study of the equilibrium shapes of anisotropic solids into anisotropic fracture: contrary to the common intuition for the fracture of crystals, cleavage planes (cusps in the G_c^{-1} curve) may in principle exist without forbidden orientations (nonconvexity). As an example taken from equilibrium crystal shapes, silicon crystals at 1373 K have facets but rounded edges and no forbidden orientation [28]. Conversely, forbidden orientations are not necessarily due to a nearby cleavage plane, but to nonconvex parts in the G_c^{-1} curve, which does not imply a large difference in fracture energy. We expect these findings to hold in the more general case of three-dimensional fracture.

We now compare this geometrical framework to experiments. For each tearing direction α, we plot on Fig. 4(a) and 4(b) the energy release-rate line for the force F measured and on this line the point with the polar angle θ of propagation. According to Griffiths criterion, (1) these points lie on the G_c^{-1} curve. The criterion for the selection of the crack path (2) predicts that the line corresponding to the optimal energy release-rate is tangent to the G_c^{-1} curve at the propagation point and remains outside of it everywhere. Criterion (2) is therefore experimentally satisfied if the energy release-rate lines are tangent to the G_c^{-1} curve. This behavior is indeed observed on Fig. 4(a) for a weakly anisotropic sheet, where the G_c^{-1} curve is convex and all fracture orientations are possible. Conversely, some directions are not observed with the strong anisotropic sheet, and the corresponding fracture energies are not accessible experimentally [Fig. 4(b)]. We observe that the energy release-rate lines are on average tangent to the remaining parts, in agreement with the same criterion. However, close to the missing sector, although the experimental lines for energy release-rate are nearly tangent to the G_c^{-1} curve at the angle of propagation, they clearly intersect the curve in another location, in contradiction with global principle (2). For instance, the propagation for a loading $\alpha = 30°$ is

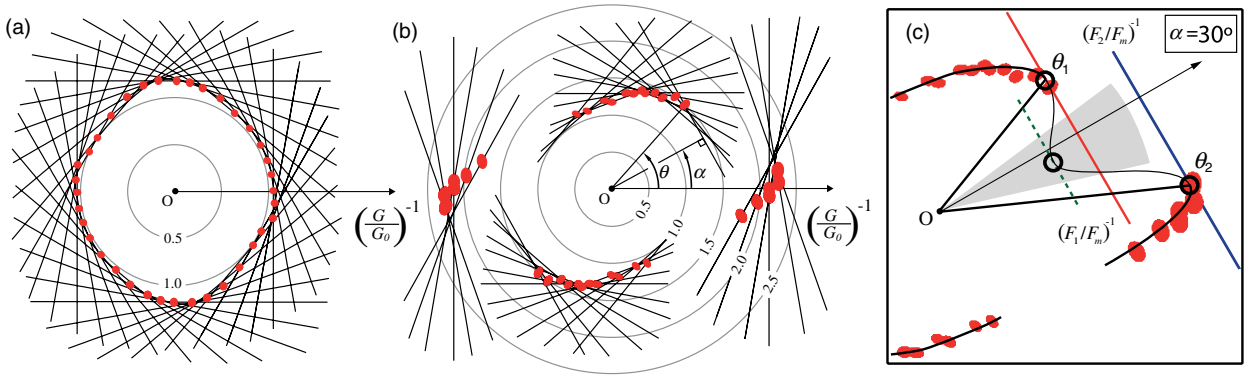

FIG. 4 (color online). Polar plots of the G_c^{-1} curves for the experiments displayed in Fig. 2. Red dots correspond to the propagation of cracks at angle θ (diameter corresponds to the estimated error) and lines to the energy release-rate measured for each experiment (α is the pulling angle). Since the fracture energy follows the symmetry $G_c(\theta + \pi) = G_c(\theta)$, only half of the orientations were actually probed. In (a) weak anisotropy, material A, and (b) strong anisotropy, material B, energy release-rate $G(\theta)$ is normalized by typical value $G_0 = 2F_m/t$ (resp. 6.6 kJ/m^2 and 6.2 kJ/m^2), where F_m is the maximal observed tearing force (resp. 0.165 and 0.156 N). In (b) the minimum measured tearing force was $0.07N$. (c) Geometrical construction [same data as in (b)], where the energy release-rate lines for $\alpha = 30°$, $\theta_1 = 51°$, and $\theta_2 = 5°$ are presented in red and blue, respectively. The G_c^{-1} curve was arbitrarily extended in light black line in the missing region where no measurement is available. The grey sector corresponds to orientations never observed even when fracture is guided (see Fig. 5).

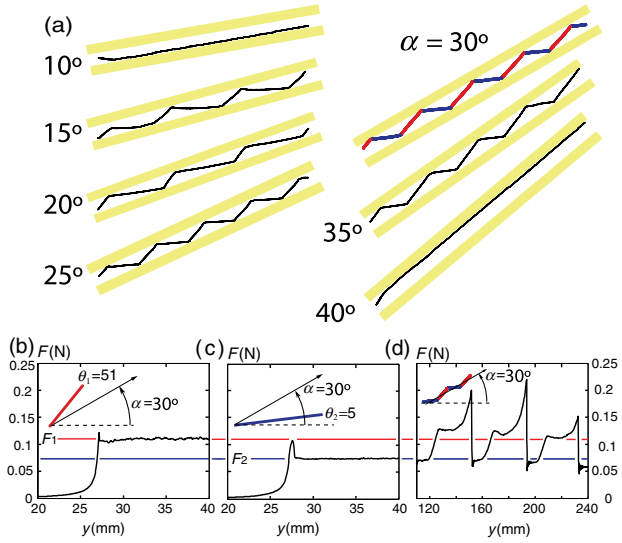

FIG. 5 (color online). Fracture guided along a forbidden direction [setup in Fig. 1(c)] in material B. A pair of adhesive tapes are placed 5 mm apart along the band of anisotropic polymer. Pulling is performed at 200 mm/min. (a) Sawtooth crack paths obtained when the crack is guided in a forbidden direction ($15° \leq \alpha \leq 35°$). When the direction is not forbidden ($\alpha = 10°, 40°$), the crack path follows one of the boundaries. (b)–(c) Measured force as function of displacement for $\alpha = 30°$, on a nonreinforced sample, in the most frequent case of propagation along $\theta = 51°$ (b), and along $\theta = 5°$ (c). (d) Force measured during zig-zag propagation ($\alpha = 30°$) in a reinforced sample. The plateaus corresponding to propagation are consistent with measurements in (b) and (c).

often observed along an angle θ_1 for a force F_1 [red line on Fig. 4(c)], whereas the maximization criterion (2) would predict a propagation for a lower load F_2, along θ_2. Nevertheless, propagation along θ_2 [blue line on Fig. 4(c)] is also observed for the same configuration, but less frequently. The selection of the angle seems to depend on imperfections of the initial cut.

Can we force tearing cracks to propagate in these missing directions? By limiting a band of anisotropic polypropylene film with two stiffer adhesive tapes, we can guide the propagation in the loading direction, α [Fig. 5(a)]. If the material were isotropic, the crack should follow the natural straight path along $\theta = \alpha$, ignoring the reinforcement. In the case of the weakly anisotropic material, the propagation is in general deflected and the crack path eventually hits and follows the reinforced boundary. Using this technique in the strongly anisotropic case, we observe some previously missing directions, which we interpret as metastable [35]. But in some directions, which we will denote forbidden directions, we observe that the crack bounces from the boundary and selects a very different direction. This direction is followed for a long distance, most of the time until the opposite boundary is hit. This kinking mechanism repeats successively, leading to a sawtooth pattern [see scanned fracture path in Fig. 5(a)] where the crack path avoids the forbidden direction. We could not devise a way to drive fracture along such forbidden directions.

All along the crack path the energy release-rate follows the same equation (3), independent from the history of the crack: the existence of sawtooth solutions shows that two stable orientations are selected from the same geometry of loading. In addition, we observe that these directions of propagation are again obtained with very different forces F_1 and F_2 as seen in Figs. 5(b) and 5(d). These observations contradict the criterion (2), which predicts propagation in the direction of global minimal force (i.e., maximum G/G_c). Both selected directions $\theta_{1,2}$ seem, however, to correspond to local angular minima of the force [the red and blue lines are locally tangent to the G_c^{-1} curve in Fig. 4(c)]. We therefore suggest that the global maximization principle should be taken in a less restrictive sense: fracture propagates in a direction that locally maximizes $G/G_c(\theta)$ (and minimizes the fracturing force). Such a criterion is compatible with our experiments and also reduces to the MERR criterion (and therefore to PLS) in isotropic cases. As a consequence, stable propagation corresponds to all portions of the G_c^{-1} curve that are locally convex. Only the points where $s(\theta) < 0$ should be considered as forbidden. In the case of strong anisotropy, the force Eshelby balance criterion is bound to give several directions for a given loading configuration [three solutions marked as black bullets in Fig. 4(c)]. Some of these directions are local maxima of the force (green dotted tangent line), where $s(\theta) < 0$, and should be discarded. The other directions are local minima of the applied force, and we suggest that they should all be considered as acceptable directions of propagation. Which of these directions is selected in a particular experiment? Our modified criterion is similar to accepting the metastable states of the faceting transition. In first-order transitions, multiple solutions (stable and metastable sates) are indeed observed, depending on the history of the system. We speculate that, in the case of fracture, the history and preparation of the system selects among possible directions of propagation.

Conclusion.—Cracks propagate as soon as they can, for the lowest possible load. We have shown that this commonly accepted extension of criterion for crack propagation in anisotropic sheets leads to features first introduced in the study of anisotropic surface tension in crystals such as facets and forbidden directions. This construction suggests that the existence of forbidden crack orientations is intimately connected with a negative fracture stiffness, $G_c''(\theta) + G_c(\theta) < 0$. Our tearing experiments support these predictions. We have indeed observed that tearing paths avoid some orientations in strongly anisotropic polymer sheets, although they do not exhibit a preferred cleavage plane. However, we found some surprising examples where cracks repeatedly chose to follow a hard path while an easier one (corresponding to a lower load) was available, which challenges the accepted theory of fracture.

We therefore suggest a less restrictive local principle: cracks may choose a direction that requires the lowest force compared to their neighboring directions. This principle allows for multiple directions. More experimental and theoretical efforts will be needed to confirm, clarify, or reject this modification of the fundamental principle of fracture mechanics and its extension to classical three-dimensional fracture.

We thank S. Akamatsu, S. Bottin-Rousseau, G. Faivre, V. Hakim, A. Karma, V. Lazarus, C. Maurini, J.-J. Marigo, and R. Schroll for useful discussions. A. Takei was supported by Research Fellowships of the Japan Society for the Promotion of Science (JSPS) for Young Scientists. This research was partially funded by CNRS-CONICYT No. 107, No. 171, and No. 548, ECOS C12E07, and Fondecyt No. 1110584.

*benoit.roman@espci.fr

[1] L. F. Pease, P. Deshpande, Y. Wang, W. Russel, and S. Chou, Nat. Nanotechnol. **2**, 545 (2007).
[2] E. Hamm, P. Reis, M. Leblanc, B. Roman, and E. Cerda, Nat. Mater. **7**, 386 (2008).
[3] B. Audoly, P. M. Reis, and B. Roman, Phys. Rev. Lett. **95**, 025502 (2005).
[4] B. Roman, P. M. Reis, B. Audoly, S. De Villiers, V. Viguié, and D. Vallet, C. R. Mec. **331**, 811 (2003).
[5] T. Tallinen and L. Mahadevan, Phys. Rev. Lett. **107**, 245502 (2011).
[6] A. Ghatak and L. Mahadevan, Phys. Rev. Lett. **91**, 215507 (2003).
[7] T. Wierzbicki, K. A. Trauth, and A. G. Atkins, J. Appl. Mech. **65**, 990 (1998).
[8] D. Sen, K. Novoselov, P. Reis, and M. Buehler, Small **6**, 1108 (2010).
[9] E. Bayart, A. Boudaoud, and M. Adda-Bedia, Phys. Rev. Lett. **106**, 194301 (2011).
[10] A. Griffith, Phil. Trans. R. Soc. A **221**, 163 (1921).
[11] L. Freund, *Dynamic Fracture Mechanics* (Cambridge University Press, Cambridge, England, 1990).
[12] R. Goldstein and R. Salganik, Int. J. Fract. **10**, 507 (1974).
[13] F. Erdogan and G. Sih, J. Basic Eng. **85**, 519 (1963).
[14] B. Cotterell and J. Rice, Int. J. Fract. **16**, 155 (1980).
[15] M. Amestoy and J.-B. Leblond, Int. J. Solids Struct. **29**, 465 (1992).
[16] A. Chambolle, G. Francfort, and J.-J. Marigo, J. Mech. Phys. Solids **57**, 1614 (2009).
[17] M. Marder, Europhys. Lett. **66**, 364 (2004).
[18] V. Hakim and A. Karma, Phys. Rev. Lett. **95**, 235501 (2005).
[19] V. Hakim and A. Karma, J. Mech. Phys. Solids **57**, 342 (2009).
[20] Although plastic dissipation results in a large fracture energy $G_c \sim 5$ kJ/m^2, the process zone is much smaller than the thickness, as can be checked with an optical microscope.
[21] R. O' Keefe, Am. J. Phys. **62**, 299 (1994).
[22] See Supplemental Material at http://link.aps.org/supplemental/10.1103/PhysRevLett.110.144301 for justification of this assumption.
[23] A. Azhdari, S. Nemat-Nasser, and J. Rome, Int. J. Fract. **94**, 251 (1998).
[24] R. D. Deegan, S. Chheda, L. Patel, M. Marder, H. L. Swinney, J. Kim, and A. de Lozanne, Phys. Rev. E **67**, 066209 (2003).
[25] D. Hull, *Fractography: Observing, Measuring and Interpreting Fracture Surface Topography* (Cambridge University Press, Cambridge, England, 1999).
[26] C. Herring, Phys. Rev. **82**, 87 (1951).
[27] N. Cabrera, Surf. Sci. **2**, 320 (1964).
[28] P. Müller and J. J. Métois, Thin Solid Films **517**, 65 (2008).
[29] C. Rottman and M. Wortis, Phys. Rep. **103**, 59 (1984).
[30] H. Jeong and E. Williams, Surf. Sci. Rep. **34**, 171 (1999).
[31] P. Müller and A. Saúl, Surf. Sci. Rep. **54**, 157 (2004).
[32] A. Dequidt and P. Oswald, Eur. Phys. J. E **19**, 489 (2006).
[33] P. Galatola, J. B. Fournier, and G. Durand, Phys. Rev. Lett. **73**, 2212 (1994).
[34] P. Oswald, F. Melo, and C. Germain, J. Phys. (Paris) **50**, 3527 (1989).
[35] Due to the extra rigidity of the reinforcement, force measurements do not allow us to characterize accurately the fracture energy of metastable orientations in Figs. 4(b) and 4(c).